

Multiple Histogram Method for Quantum Monte Carlo

C. L. Martin*

Physics Department, University of California, Santa Barbara, CA 93106

(February 1, 2008)

An extension to the multiple-histogram method (sometimes referred to as the Ferrenberg-Swendsen method) for use in quantum Monte Carlo simulations is presented. This method is shown to work well for the 2D repulsive Hubbard model, allowing measurements to be taken over a continuous region of parameters. The method also reduces the error bars over the range of parameter values due the overlapping of multiple histograms. A continuous sweep of parameters and reduced error bars allow one to make more difficult measurements, such as Maxwell constructions used to study phase separation. Possibilities also exist for this method to be used for other quantum systems.

PACS Numbers: 02.70.Lq, 71.10.Fd, 02.50.Ng, 02.60.Gf

I. INTRODUCTION

When making calculations using the Monte Carlo method, one often would like to make measurements of some observable as a function of the parameters of the hamiltonian. To do this the standard procedure is to perform a run at one setting of the parameters until a measurement of the observable with sufficiently small error bars is produced. One then moves on to another setting of the parameters, and so on until a large discrete set of measurements of the observable is produced. This can require large amounts of computer time depending on the details of the hamiltonian and the Monte Carlo method one has chosen. Building an approximation of a continuous function for the desired observable point by point would require an even larger set of discrete points, and a related increase in computer time.

Continuous functions of observables are useful for innumerable activities, such as verifying functional dependencies and looking for phase separation using Maxwell constructions.¹ The multiple histogram method² (MHM) allows one to produce these continuous functions for a classical hamiltonian. In this paper, it will be shown that under certain circumstances the MHM can also be applied to quantum mechanical hamiltonians as well, for example the two-dimensional Hubbard model.³ Observables of this hamiltonian will be measured using standard quantum Monte Carlo (QMC) techniques⁴ and the MHM will be applied to obtain observables as continuous functions of the parameters of the system. As in the classical case, the use of overlapping histograms reduces the errors below those of a single measurement. Furthermore, the MHM will be applied specifically to the density and energy of the Hubbard model as functions of the chemical potential to search for signs of phase separation.

II. SINGLE HISTOGRAM METHOD

In order to obtain a variable as a continuous function of thermodynamic variables like the inverse temperature, $\beta = (k_B T)^{-1}$, and the chemical potential, μ , one can use a technique originally used by Salsburg *et al.*,⁵ extended by Valleau and Card,⁶ and further extended by Swendsen and Ferrenberg.^{2,7} To see how this can be done for the chemical potential, μ , let us assume we have a classical hamiltonian,

$$\mathcal{H} = E - \mu n, \quad (1)$$

where E is the energy and n is the particle density. From this hamiltonian, one can derive a partition function for a particular value of μ ,

$$Z_\mu = \sum_n \rho(n) e^{\beta \mu n}, \quad (2)$$

where $\rho(n)$ is a density of states which for these purposes we can leave undetermined. We can also derive a probability to have a given density for this value of μ ,

$$P_\mu(n) = \frac{\rho(n) e^{\beta \mu n}}{Z_\mu}. \quad (3)$$

Substituting Eqn. 2 into Eqn. 3 allows us to find the probability for a value of n at a different value of the chemical potential, μ' ,

$$P_{\mu'}(n) = \frac{P_\mu(n) e^{\beta(\mu' - \mu)n}}{\sum_n P_\mu(n) e^{\beta(\mu' - \mu)n}}. \quad (4)$$

Eqn. 4 can be extended for use with many histograms taken at varying parameters, as discussed by Ferrenberg and Swendsen.² Using multiple histograms allows one to increase the range of validity of the technique.

*email: chris@physics.ucsb.edu

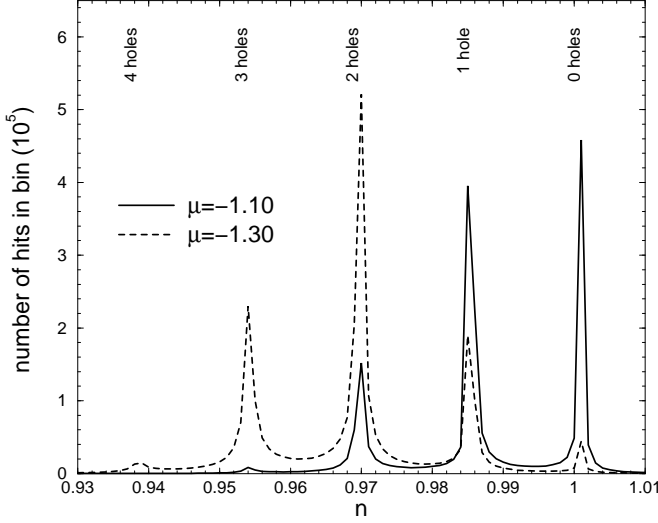


FIG. 1. A histogram of the particle density sampled after each sweep in a Quantum Monte Carlo simulation of the Hubbard model on a 8 by 8 lattice with $\beta t = 8$, $U/t = 8$, and $\mu = -1.10$ and -1.30 . One can see well defined peaks at particle densities corresponding with integer numbers of holes. It is also possible to see how the two histograms at different parameters overlap each other, allowing one to be normalized with respect to the other.

To demonstrate the use of this method for quantum hamiltonians, the Hubbard hamiltonian³ will be used

$$\begin{aligned}
 H = & -t \sum_{\langle ij \rangle} \sum_{\sigma=\{\uparrow\downarrow\}} \left(\hat{c}_{i\sigma}^\dagger \hat{c}_{j\sigma} + \hat{c}_{j\sigma}^\dagger \hat{c}_{i\sigma} \right) \\
 & + U \sum_i \left(\hat{n}_{i\uparrow} - \frac{1}{2} \right) \left(\hat{n}_{i\downarrow} - \frac{1}{2} \right) \\
 & - \mu \sum_i (\hat{n}_{i\uparrow} + \hat{n}_{i\downarrow}),
 \end{aligned} \quad (5)$$

where t is a parameter to set the strength of electron hopping (kinetic energy), $\hat{c}_{i\sigma}^{(\dagger)}$ is the annihilation (creation) operator for an electron at site i with spin $\sigma = \{\uparrow\downarrow\}$, U is a parameter to set the strength of on-site coulomb repulsion, μ is the chemical potential, and $\hat{n}_{i\sigma} = \hat{c}_{i\sigma}^\dagger \hat{c}_{i\sigma}$. Clearly there are quantum operators in the Hubbard hamiltonian, so the classical derivation given earlier for the probability as a function of μ will only hold if the system happens to be in states of definite particle number. In determinantal QMC, a Hubbard-Stratonovich (HS) transformation⁸ leads to a bilinear fermion form for the interaction. One sums over all possible fermion states and then over the HS field. Thus a given HS configuration comes from a trace over all particle numbers so that it is not guaranteed that a given HS configuration will have a definite particle number. It is this feature that distinguishes this problem from the classical statistical mechanics problem. However if one finds that the various HS configurations are indeed characterized by

an integer fermion occupation, then as we will discuss, one can proceed. Here for the 2D Hubbard model near half-filling, the charge gap provides an energy barrier to non-integer filling. As can be seen in Fig. 1, when one runs simulations at a sufficiently low temperature, one observes peaks in the histogram corresponding to states with integer numbers of holes. If these states truly have a definite number of particles, the peaks should scale using the grand canonical distribution for runs at different values of μ . In Fig. 2, such a test is performed and the peaks do scale with the grand canonical distribution as desired.

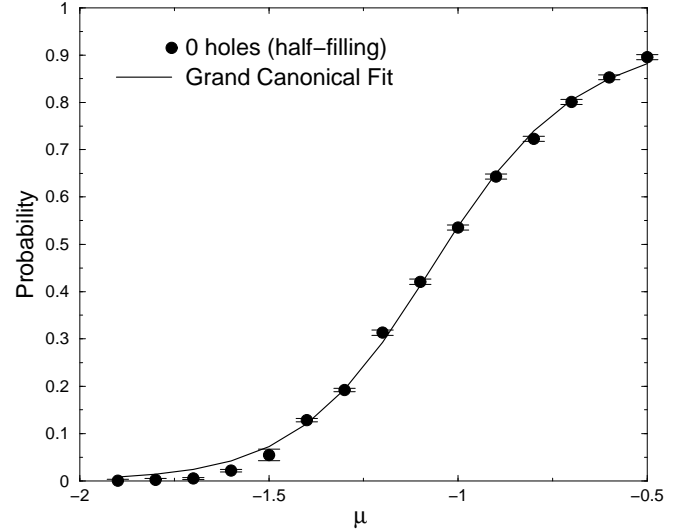


FIG. 2. Normalizing the peaks in histograms such as the ones shown in Fig. 1, yield the probability for a certain particle density. One can then change the μ used in the simulation and follow the relative probability of this peak as a function of μ . If the states truly have a definite particle density they should follow a curve given by the grand canonical distribution which is shown in the solid line.

Note that in Fig. 1, multiple histograms are presented in order to emphasize the fact that the MHM allows one to obtain even more information when several histograms are used. By normalizing each histogram with respect to the others, a continuous function of the desired observable may be obtained. In the results that follow, we have used many overlapping histograms in order to fully cover the range of simulation variables of interest.

In parameter regimes⁹ where these peaks are present in the histograms of particle number, one can proceed to take any operator that conserves particle density and determine its behavior as a continuous function of μ . This can be done by using a reduced number of simulations at different values of μ , as long as the respective histograms of particle density overlap. To prevent unwanted overlap from very distant histograms, it was found necessary to introduce a Gaussian cutoff. The cutoff reduces the effective weight of a histogram as the difference between

the value of μ for that histogram and the value of μ' at which the MHM method is run increases. As an added benefit, the error bars for this continuous function of μ will be reduced from those obtained from any one simulation, because one can use information about the operator from all of the simulations performed.

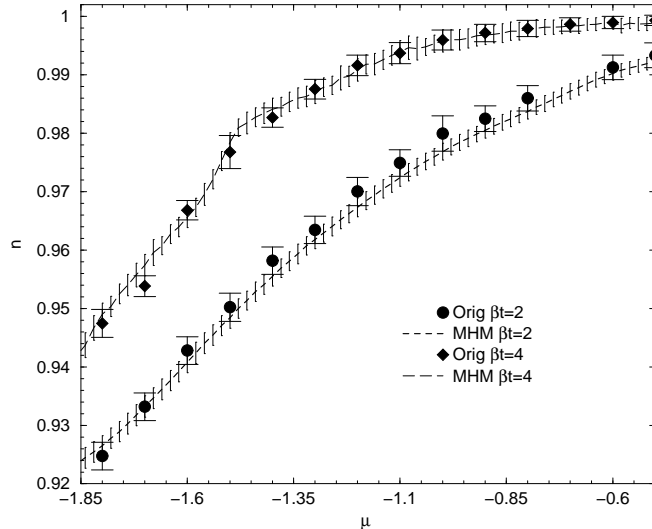


FIG. 3. The original points and the MHM method continuous curves are shown for the particle density (n) vs. chemical potential (μ) for two values of the inverse temperature, β . All simulations are performed on an 8 by 8 square lattice at $U/t = 8$. Error bars on the original data points are shown as bars with hats originating from the points, and error bars on the MHM line are shown as bars without hats originating at regular intervals from the dashed line.

III. RESULTS

In Fig. 3 one can see what happens when the Multiple Histogram Method (MHM) is applied to a set of histograms measuring the particle number during a QMC simulation of the Hubbard model. The chemical potential, μ , is varied over a range starting from half-filling ($\mu = 0$ and thus $n = \langle \hat{n} \rangle = 1$) through increasingly negative values of μ . The individual runs are shown as points with associated error bars, and the MHM is applied to get a continuous function of n vs. μ with error bars shown as vertical bars around the dashed line. The error bars are checked through both the bootstrap method¹⁰ and by incorporating the errors due to correlations in the reweighted samples and their finite size.¹¹ To see how the line changes with different values of the inverse temperature, β , the process is repeated at $\beta t = 4$.

As one can see, the error bars on the MHM line are comparable to those from the original points, and the MHM continuously fits the original points. As the simulation temperature decreases (large β) the sign problem¹² becomes much more severe. For the histogram method this means that while there are peaks in the histograms

for n vs. μ for configurations with positive signs, they are wiped out by nearly identical peaks with negative signs.

In Fig. 4, the MHM is applied to another interesting observable, the equal time antiferromagnetic spin correlation function, $S^{zz}(\pi, \pi)$, the Fourier transform of $\langle (n_{i\uparrow} - n_{i\downarrow})(n_{j\uparrow} - n_{j\downarrow}) \rangle$ taken at momentum (π, π) . As the system moves closer to half-filling ($\mu = 0$), the antiferromagnetic order increases as expected.¹³

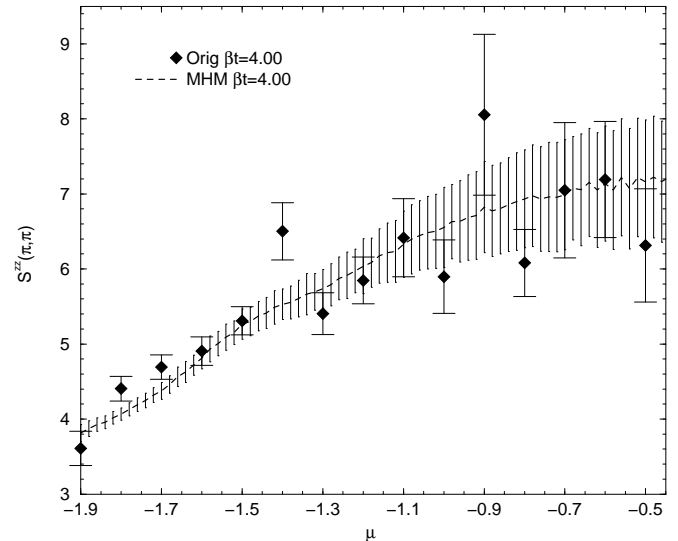


FIG. 4. Original points and the resulting MHM method continuous curve are shown for the equal time zz antiferromagnetic spin correlation function ($S^{zz}(\pi, \pi)$). As the parameters are moved closer to half-filling ($\mu = 0$), the system begins to develop antiferromagnetic order as shown by the increasing value of $S^{zz}(\pi, \pi)$. The simulations are performed on an 8 by 8 square lattice at $U/t = 8$. Error bars on the original data points are shown as bars with hats originating from the points, and error bars on the MHM line are shown as bars without hats originating at regular intervals from the dashed line.

IV. PHASE SEPARATION

Recently, computational evidence for the existence of phase separation in the strongly correlated t-J and Hubbard models, both for and against, have been presented in the literature.¹⁴ One of the best ways to search for phase separation is through the use of a Maxwell construction.¹ A Maxwell construction consists in its simplest form as a graph of energy vs. density. Thermodynamics wants a system to minimize its free energy, and so a phase separated region will appear on the graph as a region of upwards curvature ($\frac{\partial^2 E}{\partial n^2} < 0$). In such a region the energy of the phase separated state will be lower than that of the homogeneous state, and phase separation is thus favored. It is of interest, therefore, to apply the MHM to obtain continuous energy versus density measurements in order to investigate the possible existence of phase separation. In Fig. 5, a Maxwell construction for the 2D Hubbard

model at $\beta t = 4$ is shown. With just the original data points it is nearly impossible to say anything definitive about the curvature of the line, however when the MHM method is employed, the lack of any clear signs of upwards curvature becomes much more apparent. Thus it is possible to conclude that one does not see phase separation for this range of parameters, a conclusion that would have been difficult to make without using the full information from the histograms.

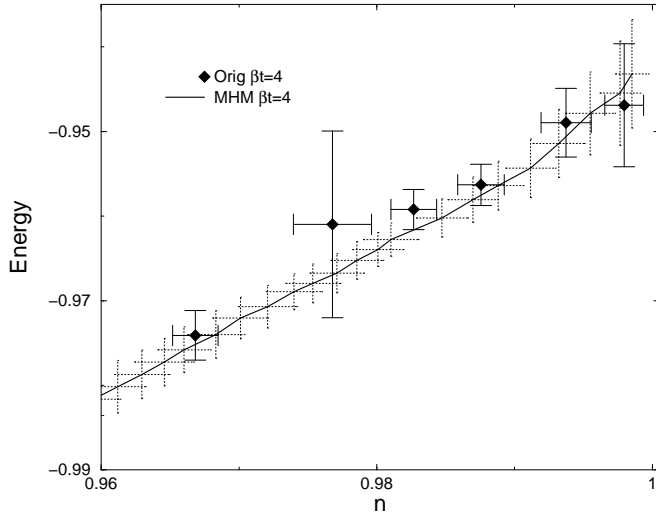


FIG. 5. Original points and the resulting MHM method continuous curve are shown for a Maxwell construction of energy vs. particle density (n); some points have been omitted for clarity. Phase separation would be indicated by a region of the curve with upwards curvature, which appears in neither curve. Error bars for both the uncertainty in energy and particle density on the original data points are shown as bars with hats originating from the points, and error bars on the MHM line are shown as dotted bars without hats originating from the dashed line.

V. CONCLUSIONS

In some circumstances, the MHM method can be used effectively for hamiltonians containing quantum operators, such as the Hubbard hamiltonian just described. The ability to generate continuous functions of an observable makes a number of analysis techniques much more feasible. For example, in order to perform a Maxwell construction,¹ a continuous function of energy as a function of particle density is desired. Previously a function like this would have been constructed laboriously one point at a time using the averages of large simulations, and conclusions drawn using reasonable guesses about what function would fit the calculated points. Using the multiple histogram method, the large quantity of information present in the histograms of each simulation is brought to bear using simple statistical physics

arguments. The information from the simulations is thus used more efficiently and smaller error bars and reasonable continuous functions are produced.

VI. ACKNOWLEDGEMENTS

Support was received from the US Department of Energy under Grant No. DE-FG03-85ER45197, and computer time on the Cray T90 at SDSC was provided by NPACI. Useful discussions and insights were generously provided by D. Scalapino, R. Sugar, D. Duffy, and E. Kim.

-
- ¹ K. Huang, in *Statistical Mechanics*, 2 ed. (John Wiley & Sons, Inc., New York, New York, 1987), pp. 41–3,163–7.
 - ² A. Ferrenberg and R. Swendsen, Phys. Rev. Lett. **63**, 1195 (1989).
 - ³ J. Hubbard, Proc. Royal Soc. London A **276**, 238 (1963).
 - ⁴ R. Blankenbecler, D. Scalapino, and R. Sugar, Phys. Rev. D **24**, 2278 (1981); J. Hirsch, Phys. Rev. B **31**, 4403 (1985); S. White *et al.*, Phys. Rev. B **40**, 506 (1989).
 - ⁵ Z. W. Salsburg, J. D. Jacobson, W. Fickett, and W. W. Wood, J. Chem. Phys. **30**, 65 (1959).
 - ⁶ J. Valleau and D. Card, J. Chem. Phys. **57**, 5457 (1972).
 - ⁷ A. Ferrenberg and R. Swendsen, Phys. Rev. Lett. **61**, 2635 (1988), *Erratum* **63**, 1658 (1989); R. Swendsen, Computer Physics Communications **65**, 281 (1991); R. Swendsen, Physica A **194**, 53 (1993); A. Ferrenberg, D. Landau, and R. Swendsen, Phys. Rev. E **51**, 5092 (1995).
 - ⁸ J. Hirsch, Phys. Rev. B **28**, 4059 (1983).
 - ⁹ For values of $U/t \gtrsim 12$, Scalettar *et al.* [Phys. Rev. B **44**, 10502 (1991)] found that determinant QMC calculations, such as the ones being performed here, fail to explore the phase space ergodically and the simulations become trapped at single values of the density, n . The simulations described here for $U/t = 8$, clearly sample (see Fig. 1) multiple values of n , and do not have this problem.
 - ¹⁰ B. Efron and G. Gong, Am. Stat. **37**, 36 (1983).
 - ¹¹ M. E. J. Newman and R. G. Palmer, cond-mat/9804306 (unpublished).
 - ¹² E. Loh, Jr., J. Gubernatis, R. Scalettar, S. White, D. Scalapino, and R. Sugar, Phys. Rev. B **41**, 9301 (1990).
 - ¹³ J. Hirsch and S. Tang, Phys. Rev. Lett. **62**, 591 (1989).
 - ¹⁴ C. Au and B.-H. Zhao, cond-mat/9602054 (unpublished); M. Simon and A. Aligia, Phys. Rev. B **53**, 15327 (1996); G. Su, Phys. Rev. B **54**, 8281 (1996); E. Ercolessi, P. Pieri, and M. Roncaglia, Phys. Lett. A **233**, 451 (1997); C. Hellberg and E. Manousakis, Phys. Rev. Lett. **78**, 4609 (1997); M. Kohno, Phys. Rev. B **55**, 1435 (1997); A. C. Cosentini, M. Capone, L. Guidoni, and G. B. Bachelet, cond-mat/9801299 (unpublished).